Front. Earth Sci. 2022, 16(1): 206–219
https://doi.org/10.1007/s11707-021-0872-2

RESEARCH ARTICLE

Short-fetch high waves during the passage of 2019 Typhoon Faxai over Tokyo Bay

Hiroshi TAKAGI (✉), Atsuhei TAKAHASHI

School of Environment and Society, Tokyo Institute of Technology, Tokyo 152-8550, Japan

Abstract The risk of wind waves in a bay is often overlooked, owing to the belief that peninsulas and islands will inhibit high waves. However, during the passage of a tropical cyclone, a semi-enclosed bay is exposed to two-directional waves: one generated inside the bay and the other propagated from the outer sea. Typhoon Faxai in 2019 resulted in the worst coastal disaster in Tokyo Bay in the last few decades. The authors conducted a post-disaster survey immediately after this typhoon. Numerical modeling was also performed to reveal the mechanisms of unusual high waves. No significant high-wave damage occurred on coasts facing the Pacific Ocean. By contrast, Fukuura-Yokohama, which faces Tokyo Bay, suffered overtopping waves that collapsed seawalls. To precisely reproduce multi-directional waves, the authors developed an extended parametric typhoon model, which was embedded in the JMA mesoscale meteorological model (JMA-MSM). The peak wave height was estimated to be 3.4 m off the coast of Fukuura, in which the contribution of the outer-sea waves was as low as 10%–20%. A fetch-limited wave developed over a short distance in the bay is considered the primary mechanism of the high wave. The maximum wave occurred on the left-hand side of the typhoon track in the bay, which appears to be contrary to the common understanding that it is safer within the semicircle of a storm than on the opposite side. Typhoon Faxai was a small typhoon; however, if the radius was tripled, it is estimated that the wave height would exceed 3 m over the entire bay and surpass 4 m off the coasts of Yokohama and Chiba.

Keywords Typhoon Faxai, Tokyo Bay, high waves, short fetch, overtopping, wave hindcasting, parametric typhoon, JMA-MSM, storm surge

Received August 18, 2020; accepted January 5, 2021

E-mail: takagi@ide.titech.ac.jp

1 Introduction

In the metropolitan area of Japan, two out of the ten most populated regions in the world are located — the Greater Tokyo (#1) and Greater Osaka (#10) regions, with a total population of 37 million and 19 million, respectively (United Nations, 2018). Both cities are situated in semi-closed bays, steadily expanding over the last several centuries. The natural breakwater system by the peninsulas and the inner-bay islands greatly contributed to the creation of a calm waterfront, providing huge benefits for human society, particularly for industrial development. However, both Tokyo Bay and Osaka Bay recently experienced the severe impact of strong typhoons. Typhoon Jebi hit Osaka Bay on September 4, 2018, causing severe damage to Greater Osaka, Japan's second-largest economic region. In addition to the impact on urban infrastructure over the broad areas along the path of the typhoon, the strong winds generated high waves and storm surges, resulting in historical economic damage (approximately 168 million US dollars) on the port and coastal infrastructure (Fig. 1(a)) (Takabatake et al., 2018; Le et al., 2019; Mori et al., 2019).

On September 9, 2019, Typhoon Faxai hit Greater Tokyo, the nation's largest economic region, and proceeded directly above Tokyo Bay. Although the storm surge was relatively minor, locally concentrated waves caused significant damage in a particular area on the western shore of Tokyo Bay (Suzuki et al., 2020). As a consequence of the failure of the coastal dike (Fig. 1(b)), an industrial zone in Yokohama was extensively flooded, resulting in the suspension of several hundred factories. Typhoon Faxai caused the greatest coastal disaster in Tokyo Bay since the development of the waterfront in Japan's high-growth period (the mid-1950s to the early-1970s) (Takagi et al., 2020a; Yamamoto et al., 2020). Tokyo Bay consists of an inner bay and an outer bay, and has a total area of 1380 km^2 (in this study, the inner bay is mainly focused). The bay mouth separating the inner from the outer bay is only 7 km apart at its narrowest section.

(a) (b)

Fig. 1 (a) Failure of the coastal dike in Osaka, caused by high waves due to 2018 Typhoon Jebi (photo taken by the author); (b) Damage in Yokohama, due to 2019 Typhoon Faxai (photo courtesy of Port & Harbor Bureau, City of Yokohama).

The risk of high waves is often overlooked because it is believed that two peninsulas work as an effective natural breakwater (Solomon, 2016). However, a remarkably high wave was generated when Faxai proceeded over the bay. Table 1 shows the rank of the high wave observed at Tokyo Port, demonstrating that the wave recorded during Faxai was the highest over the past five decades. A wave over 3 m is not necessarily rare in the Pacific Ocean; however, it has taken place only three times in Tokyo Bay in the past four decades. The other two high-wave events were also caused by typhoons, Irma in 1985 and Danas in 2001. Irma may not simply be compared with Faxai, as Irma did not take the course above Tokyo Bay. However, Danas and Faxai proceeded in a similar route over Tokyo Bay at the same speed. According to Islam and Takagi (2020a), the average forward speed of past typhoons, which impacted Tokyo Bay, was estimated to be 46 km/h. Thus, these two typhoons moved slowly at approximately half the speed of the averaged typhoon. In terms of size, Faxai and Danas can be classified as small typhoons, with the 50-knot wind speed radius (R50) being smaller than 100 km (Table 1).

A slow-moving, small typhoon would have a different impact on storm surge in the bay compared with a fast-moving, large typhoon. A recent statistical study using long-term tidal records suggests that fast-moving typhoons tend to amplify storm surges in open coasts but reduce them in semi-enclosed bays (Islam and Takagi, 2020b). The amplification of storm surges may also be pronounced through resonance mechanisms when coinciding with atmospheric disturbances, such as gravity waves, frontal passages, pressure jumps, and squalls, with similar periods in long waves such as storm surges (Monserrat et al., 2006), sometimes leading to devastating currents (Heidarzadeh and Rabinovich, 2020).

However, the mechanism of wave intensification is not necessarily the same as that of storm surges. The growth of wind waves has been extensively studied for at least a century. In the early days, field data of ocean waves were collected on ships using visual inspection, contributing to the determination of a relationship between wind speed, wave height, and wave period. Stevenson (1874) proposed a simple prediction of wave height that is solely proportional to the square root of the fetch; meanwhile, Molitor (1935) introduced wind speed into an empirical wave-forecasting formula. The modern study of ocean surface waves started with a pioneer study by Sverdrup and Munk (1947). They proposed a forecasting method for fetch- and duration-limited waves, which was later revised by Bretschneider (1951) with the addition of much field data. Thus, their forecast is collectively called the SMB method, using the initial from each author. Wilson (1965) further advanced this empirical model by considering the development of waves during severe winter storms. Meanwhile, a statistical description of ocean waves has been investigated using a wave spectrum, since Pierson and Moskowitz (1964) proposed a spectrum shape, known as the Pierson–Moskowitz spectrum.

This spectrum was derived based on the assumption that waves will reach an equilibrium state if the wind steadily blows for a long period over a large area. However, an early wave tends to be smaller than that in a fully developed sea while containing a steep spectral peak. To consider an important mechanism to enhance the growth of early wind waves, the JONSWAP group introduced nonlinear interactions among wind-generated waves into the spectrum (Hasselmann et al., 1973). Mitsuyasu (1972) also proposed one-dimensional wave spectra for a limited fetch F, which approaches the Pierson–Moskowitz spectrum at the dimensionless fetch ($= gF/u_*^2$) of approximately 10^7 (g and u_* are the gravitational acceleration and the friction velocity of wind, respectively.).

In addition to maximum wind velocity, various factors, such as the forward speed of the system, radius of maximum wind speed, and fetch length, play important roles in determining the development of waves (Bowyer and MacAfee, 2005; Hwang and Walsh, 2018). Observa-

Table 1 Historical typhoons that hit Tokyo Bay

#	Year /Month /Day	Case TY: typhoon WS: winter storm SS: spring storm	TY name	Wave height/m	Wave period/s	Storm surge/m Harumi Station, Tokyo	Landfall location from central bay axis	Approach angle relative to coastline (degree in clockwise direction)	Forward speed at landfall /(km·h^{-1})	Radius of R50 at landfall/km	Max 10-min sustained wind speed at landfall /(m·s^{-1})
1	2019/9/9	TY	Faxai	3.39	7.1	1.01	over Tokyo Bay	135	24	93	41
2	1985/7/1	TY	Irma	3.09	4.2	1.2	80 km (southwest)	130	69	232	33
3	2001/9/11	TY	Danas	3.09	7.4	1.12	over Tokyo Bay	120	24	56	28
4	2004/12/5	WS	—	2.93	5.9	—	—	—	—	—	—
5	2007/9/6	TY	Fitow	2.55	4.7	1.04	50 km (south west)	110	23	167	33
6	2019/10/12	TY	Hagibis	2.45	5.1	1.38	50 km (south west)	130	37	333	41
7	1990/4/8	SS	—	2.31	5.7	—	—	—	—	—	—

Note: The wave heights and periods were retrieved from the wave-monitoring database of Tokyo Port, covering 1983 to 2019. The other items were taken from the paper of Islam and Takagi (2020a).

tions at monitoring stations arranged along a line in a closed lake played a critical role in investigating wind waves under fetch-limited conditions. For example, an investigation of hurricane wind patterns over Lake Okechobee in the United States contributed to the establishment of a parametric typhoon model, which is often used for storm-surge forecasting (Schloemer, 1954; Myers, 1954). The growth rate of wind waves has also been investigated in Lake St. Clair and Lake Ontario, Canada and Lake Georgy, Australia (Donelan et al., 1992; Komen et al., 1994; Young and Verhagen, 1996). Tokyo Bay covers 922 km^2 with an average depth of 17 m, of which the scale is similar to the above-mentioned lakes. Hence, studies on lakes may also be useful in investigating storm-induced waves in the bay. Unlike a lake, however, Tokyo Bay is connected to the Pacific Ocean through the entrance of a length of 7 km at the narrowest cross-section. Therefore, wind waves developed in the bay need to be investigated from the aspect of a semi-closed characteristic.

In the following section, the situation after Typhoon Faxai is briefly described, based on our post-disaster survey. Our model for typhoon and wave hindcasting is then explained with an emphasis on modeling a small typhoon. The investigation using the wave model aims to analyze the mechanisms of high waves over a short distance inside Tokyo Bay. It also aims to understand why a particular area in Yokohama was severely damaged. Revealing the mechanism of inner-bay high waves would be beneficial for planning the safe use of ports in consideration of future typhoon risks. In fact, it is difficult to construct a large seawall and breakwater at the waterside of the wharf because it hinders the operation of the port. However, it is important to anticipate the possible high-wave damage for business continuity.

2 Aftermath of Typhoon Faxai

This section briefly describes the damage observed at several coasts in Kanagawa and Chiba Prefecture, revealed through our post-disaster survey (Figs. 2 and 3). In Kanagawa (western side of Tokyo Bay), significant high-wave damage was confirmed in the port areas of Naka Ward and Kanazawa Ward, Yokohama City, directly facing Tokyo Bay. At Honmoku Wharf (**KG1**) and near Yokohama Bayside Marina (**KG2**), the fence on the revetment collapsed owing to wave overtopping. The fence fell over a wide area at **KG1**; however, at **KG2**, the damage took place at only one corner of the revetment. The seawall height at **KG2** was 2.7 m above sea level. In the Fukuura district of Kanazawa Ward, a part of the seawall on the east side collapsed, and large-scale flood damage occurred in the factory district behind the seawall owing to coastal flooding. Many factories were closed at the time of our visit. At **KG3**, the parapet collapsed (see also Fig. 1(b)), and the window glass in the public toilet broke approximately 4 m above the ground. The possibility of strong winds cannot be ruled out; however, judging from the situation in which many pieces of window glass on both the land and the seaside were broken, it was thought that the damage was most likely due to waves. As the surrounding elevation is near + 3 m, it is expected that the water mass due to wave overtopping reached as high as a mean sea level (MSL) of + 7 m behind the dike. The tide level deviation at the time of inundation was approxi-

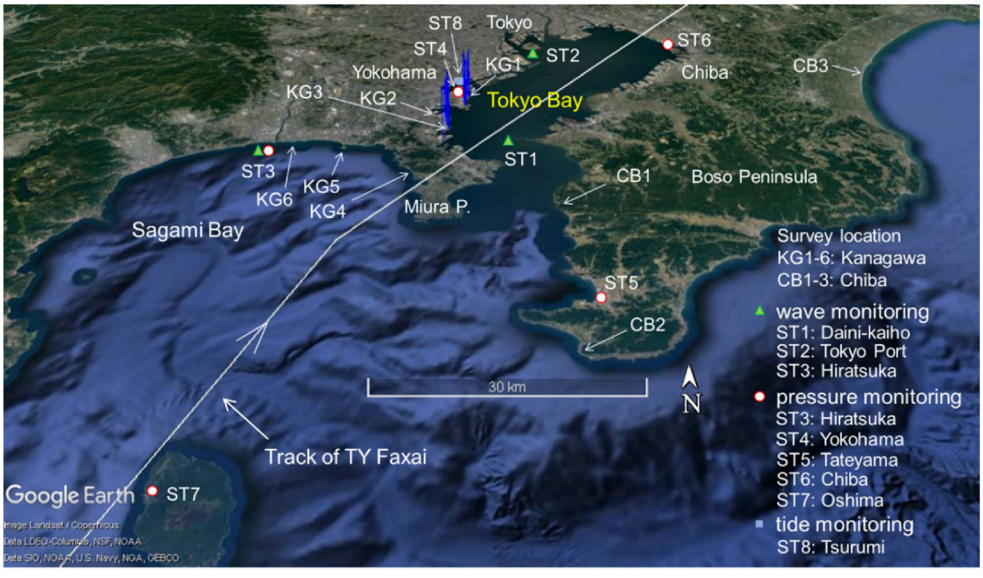

Fig. 2 Survey locations along the coast of inner and outer Tokyo Bay. Monitoring stations of waves, sea-level pressure, and tides are indicated with different symbols. Wave-overtopping took place in many locations on the western shore of Tokyo Bay (on the left side of the track of Typhoon Faxai). The blue bars show the distribution of the inundation ~5.1 m above sea level (Suzuki et al., 2020).

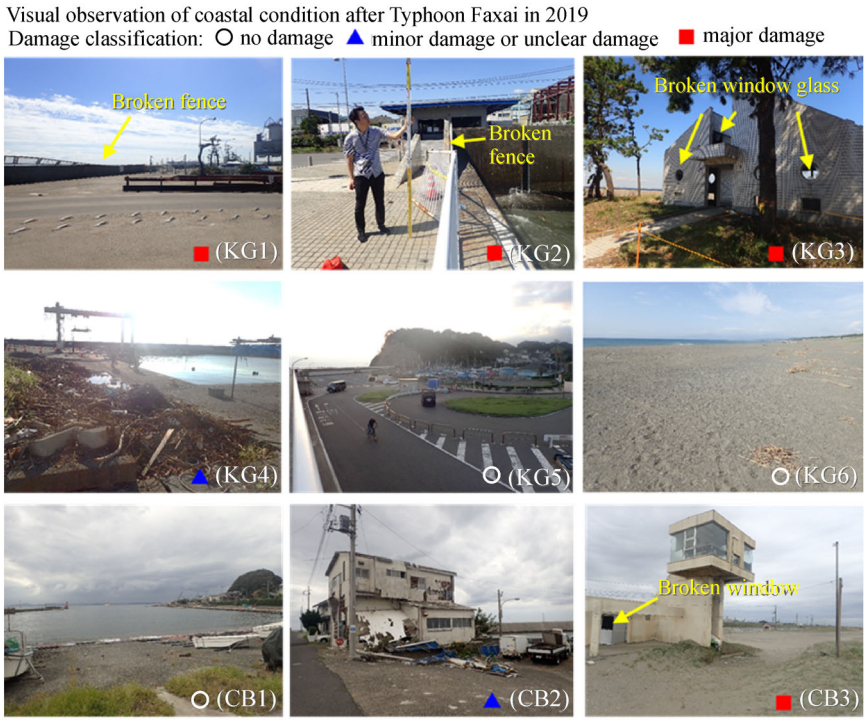

Fig. 3 Scenes after Typhoon Faxai in Kanagawa and Chiba prefecture (all photos taken by the authors). Minor damage: objects are scattered or adhered, but there is no noticeable damage to the building or structure caused by waves. Major damage: Partial or total damage to the building or structure caused by waves.

mately 0.7 m, which was not extremely high. Therefore, the main cause of the large-scale inundation was considered to be a large amount of seawater overtopped by the high waves through the collapse of the parapet.

Prior to Typhoon Faxai, Typhoon Lan in 2017 made landfall in the Kanto region and caused significant damage to the coastal areas. The authors also conducted a detailed survey of Typhoon Lan (Islam et al., 2018). Akiya Port in Yokosuka City facing Sagami Bay was damaged by Lan, and some sections of the breakwater parapet completely collapsed. However, no damage occurred due to Faxai, except the scattering of driftwood on the yard **(KG4)**. In Enoshima, no noticeable damage was confirmed (**KG5**), although this location was significantly damaged by Lan (Islam et al., 2018). Driftwood and branch trees were scattered along the coast of the Chigasaki fishing port (**KG6**). Measurements from a handy distance meter (TruPulse 360; LaserTechnology, Inc.) showed that the position was approximately 37 m from the shoreline and 1.7 m above sea level (measurement date: September 20, 9:20 UTC + 9). As the highest observed tide during the typhoon (Odawara tide station, Japan Meteorological Agency) was MSL + 1.74 m, it is estimated that the floating debris rested near the peak water level.

In Chiba (eastern side of Tokyo Bay), the roof tiles scattered, and the poles collapsed further upon approaching the southern end of the Boso Peninsula, demonstrating the ferocity of the strong winds when Faxai passed. In this way, the damage caused by strong winds was particularly prominent in a wide area in Chiba, whereas it was not so significant in Kanagawa. The seawall at Kanaya Port collapsed owing to the damage caused by the high waves during the 2017 Typhoon Lan (Islam et al., 2018). There was no noticeable damage at **CB1**, except the building damage that was caused by strong winds. In the Aihama fishing port, located on the tip of the Boso Peninsula, building damage due to wind was evident. However, it was unclear whether the high waves contributed to this damage (**CB2**). On the eastern coast of the Boso Peninsula, no major damage to the coastal infrastructure, such as dikes, breakwaters, and seawalls, was found. However, a situation was observed in which the door of the management facility at Kujukurihama Beach was breached (**CB3**). This facility was measured to be located approximately 104 m from the shoreline, and the height of the damaged window glass was 4.1 m above sea level (Sep 13, 9:30 UTC + 9). The sand adhered to the entire surface of the indoor ceiling of the facility. Thus, it was speculated that the high waves broke the door and filled the building with seawater containing a large amount of sand.

Overall, Typhoon Faxai did not damage the entire coastline of the Kanto region, but was concentrated in parts of Tokyo Bay. Hence, Typhoon Faxai may have received less attention than Typhoon Jebi in 2018 because the damage was concentrated in a smaller area.

3 Method

3.1 Weather–typhoon–hydrodynamic–wind-wave modeling

From the post-disaster survey, high-wave damage due to Faxai was found to be concentrated in Tokyo Bay. Therefore, a wave-hindcast simulation was performed, focusing on the timing at which Faxai approached Tokyo Bay and traversed the bay. Figure 4 describes the entire flow of the models. In terms of weather hindcasting, the present study uses data provided by the Japan Meteorological Agency (JMA). The JMA mesoscale numerical model (hereinafter referred to as JMA-MSM), based on non-hydrostatic and fully compressible equations, has been operated since 2004 to provide information for disaster prevention and aviation safety (JMA, 2019). The domain covers Japan and its surrounding areas (4080 km × 3300 km) with 48 vertical layers (lowest layer is 10 m above the Earth's surface). A four-dimensional variational (4D-Var) scheme is utilized as the data assimilation technique. Various observational data, such as weather radar, satellite observations, and ground-based GNSS, are used to improve the accuracy of the mesoscale model.

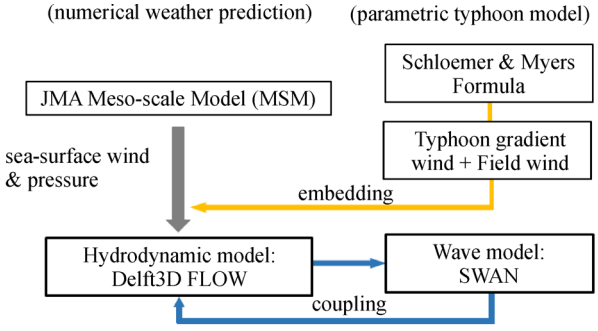

Fig. 4 Flowchart of the wave hindcasting, coupled with meteorological and hydrodynamic models.

JMA-MSM incorporates the so-called typhoon bogus model to generate a realistic typhoon structure with the assimilation technique, using pseudo-observation information (JMA, 2019). The JMA-MSM was constructed on computational grids of 5 km horizontal resolution. This model has been used as an external forcing for storm surge and has been demonstrated to be accurate (Heidarzadeh et al., 2021). The European Centre for Medium-Range Weather Forecasts (ECMWF) launched the new reanalysis data set of ERA5 in 2018, which has a horizontal resolution of approximately 30 km. The resolution of JMA-MSM is much finer than that of ERA5, whereas ERA5 covers the entire globe. However, it is still far less sufficient in precisely capturing the complex coastline of Tokyo Bay and its surrounding peninsulas. In addition, the structure of a small typhoon such as Faxai is more spatially steep than that of a large typhoon. A 5 km resolution is not able to precisely model the inner core of such a small typhoon.

To overcome the low-resolution problem, the parametric typhoon model developed by the authors was combined with background weather data of JMA-MSM to better reproduce the core of a typhoon vortex (hereinafter TY Vortex) (Fig. 4). It has been proven that the integrated parametric typhoon model and the latest mesoscale meteorological model (such as ERA5 and NCEP-CFSV2) are effective in improving the reproduction of storm surges and wind waves (Chen et al., 2019, Hsiao et al., 2020). The TY Vortex model calculates the sea-level pressure and wind fields using basic parameters (i.e., central pressure and position at each recording period), obtained from the JMA Typhoon Best Track Data. The reliability of the TY Vortex model has been verified for past strong typhoons over the Western North Pacific, such as Haiyan in 2013 (Takagi et al., 2016, 2017), Goni in 2015 (Takagi and Wu 2016), Nepartak in 2016 (Hsiao et al., 2020), and Hato in 2017 (Takagi et al., 2018).

In the TY Vortex model, the distribution of atmospheric pressure at a distance r around a typhoon's center is estimated by the following formula (Schloemer 1954; Myers 1954):

$$P(r) = P_c + \Delta P \exp\left(-\frac{r_m}{r}\right), \quad (1)$$

where ΔP, P_c, and r_m denote the pressure drop, central pressure, and radius of the maximum wind speed, respectively.

The radius r_m can be estimated from empirical formulas based on central pressure or a strong wind radius (Takagi and Wu, 2016). However, Faxai is characterized as a small typhoon. Therefore, a large error might be unavoidable, as these formulas estimate average-sized typhoons. In this study, the authors calibrated r_m to be best-fitted with the observed atmospheric pressures, rather than using an empirical formula. Because the center of the typhoon passed directly above Tokyo Bay, it is possible to simultaneously compare the JMA station data at Hiratsuka (**ST3**), Yokohama (**ST4**), Tateyama (**ST5**), Chiba (**ST6**), and Oshima (**ST7**), located on the western or eastern sides of the typhoon course (Fig. 2**)**. As a result of preliminary trials, in which the r_m was changed in 2 km increments, agreement regarding the atmospheric pressure between the calculation and observation is found to be particularly good at radius $r_m = 28$ km; thus, this value was used in this calculation.

The wind speed is calculated as the sum of two velocity components, gradient wind U_1 and background wind U_2, associated with a moving typhoon. A gradient wind is a balanced state among the Coriolis force, centrifugal forces, and radial pressure gradient force. Applying Eq. (1), the general formula of the gradient wind can be formulated as follows:

$$U_1(r) = \sqrt{\frac{r}{\rho_a}\frac{\partial P(r)}{\partial r} + \left(\frac{rf}{2}\right)^2} - \frac{rf}{2}$$

$$= \sqrt{\frac{\Delta P}{\rho_a}\frac{r_m}{r}\exp\left(-\frac{r_m}{r}\right) + \left(\frac{rf}{2}\right)^2} - \frac{rf}{2}. \quad (2)$$

It was assumed that background wind U_2 is a function of the gradient wind speed U_1 and typhoon traveling speed V:

$$U_2(r) = \frac{U_1(r)}{U_1(r_m)}V. \quad (3)$$

The conversion of wind direction and speed as a result of sea-surface friction is utilized. Similar to the conventional method, the present model assumes that the wind blows at an angle of 30° to the tangent of the typhoon vortex. A reduction in wind speed is achieved by applying a factor of 0.6 to 0.7 to Eqs. (2) and (3).

To embed TY Vortex into JMA-MSM, the square of Cressman interpolation is adopted as the weight function W (Cressman, 1959):

$$W = \left(\frac{R_B^2 - r^2}{R_B^2 + r^2}\right)^2. \quad (4)$$

R_B is the distance at which W approaches zero. Only positive values of W were used. The wind and pressure fields are solely determined by JMA-MSM where outside the radius of R_B, whereas TY-Vortex model is incorporated into JMA-MSM within R_B. In this study, R_B is assumed to be a factor of three greater than the radius r_m (i.e., $28 \times 3 = 84$ km):

$$p_{mix} = (1 - W)p_1 + Wp_2, \quad (5)$$

$$u_{mix} = (1 - W)u_1 + Wu_2. \quad (6)$$

Equations (5) and (6) calculate the blended values — pressure p_{mix} and velocity u_{mix}. Parameters p_1 and u_1 are data taken from JMA-MSM, whereas p_2 and u_2 are data from the TY-Vortex model.

Using the aforementioned typhoon field as atmospheric forcing, the wind waves can be simulated using the Simulating Waves Nearshore (SWAN) model (TU Delft, 2000). SWAN is a third-generation wave model that computes random, short-crested, and wind-generated waves in coastal regions (Booij et al., 1999). Various options can be selected for this model. The Komen model was selected for wave generation, whereas the Battjes and Janssen model was used as the breaking-wave model. It is unlikely that the wave height decreases owing to breaking waves because Tokyo Bay has few natural shallow coasts left. However, in shallow water, damping appears, owing to the oscillating flow in waves; thus, the empirical friction resistance formula called the JONSWAP bottom friction model was selected. In addition, the energy dissipation due to white capping and nonlinear wave–wave interaction was considered. The SWAN model accounts for most of the wave physics, such as wave refraction, shoaling, breaking, and dissipation. The radiation stress can also be calculated; however, the wave setup effect is hardly reflected in the simulation with a coarse grid. The Manning's n value was set to be 0.02 ($s \cdot m^{-1/3}$) throughout the computational domain for sea-bed roughness.

Simultaneously, hydrodynamic analysis was performed by the Delft 3D FLOW, and its calculation result was fed to the SWAN. The coupling time step between the two models was 60 min. The Delft3D FLOW incorporates a hydrostatic nonlinear shallow water solver that calculates non-steady flow. This model can perform both two-dimensional and three-dimensional analyses; however, in this study, a two-dimensional analysis was used. In this case, it is equivalent to the nonlinear long-wave equation model generally used for tsunami and storm surge analysis (Takagi et al., 2020b). The analysis was performed in a spherical coordinate system, and the bathymetric data provided by the G-spatial Information Center were assigned in a mesh of approximately 500 m.

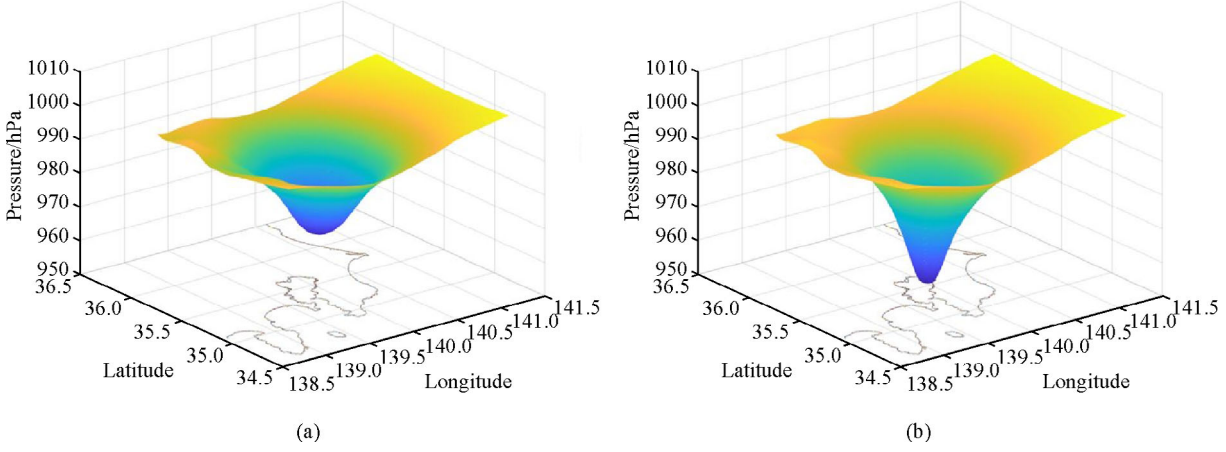

Fig. 5 Comparison of atmospheric pressure at 2:00 Sep 9 (UTC + 9): (a) only JMA-MSM, (b) JMA-MSM and TY Vortex combined model.

3.2 Model accuracy

Figure 5 shows the comparison of the estimated pressure drop by only JMA-MSM and JMA-MSM + TY Vortex. The latter model more accurately calculates a deep and steep pressure profile, which is expected to improve the accuracy of wave hindcasting. As shown in Fig. 6, the comparison with the data observed at five meteorological stations (**ST3**, **ST4**, **ST5**, **ST6**, **ST7** in Fig. 2) demonstrates a better prediction for the JMA-MSM + TY Vortex model, whereas JMA-MSM alone significantly underestimates the pressure drop at the three stations, particularly close to the typhoon track (**ST4**, **ST6**, **ST7**). In terms of waves, the observation at Daini-Kaiho (**ST1**) may well describe the wave characteristics near the bay mouth, while that at Tokyo Port (**ST2**) represents the innermost part of the bay. The JMA-MSM + TY Vortex model estimates a peak wave similar to the observation at **ST1**, whereas JMA-MSM alone substantially underestimates the wave height and period. Both models precisely estimate the wave height at 3 am. The observed height continued to increase up to nearly 3.5 m at 4 am, whereas those in the two models begin to decrease. These discrepancies can be caused by multiple factors. The low resolution of the computational grid (~500 m) may be critical, especially in the innermost bay area where the coastline is complex and the bathymetry is not smooth because of extensive dredging. The actual typhoon should have been distorted owing to significant influence from land, whereas the TY Vortex model simply assumes an idealized concentric circle.

The observation at Hiratsuka (**ST3**) in Sagami Bay is useful for observing the difference in wave characteristics between the bay and the outer sea. However, the simulation result at this location, irrespective of the model selection, significantly underestimates both the wave height and period. The observed data suggest that longer swells with a period of 12 s reached Hiratsuka. This is almost twice the wave period inside the bay. Although the present computational domain is sufficiently large to model

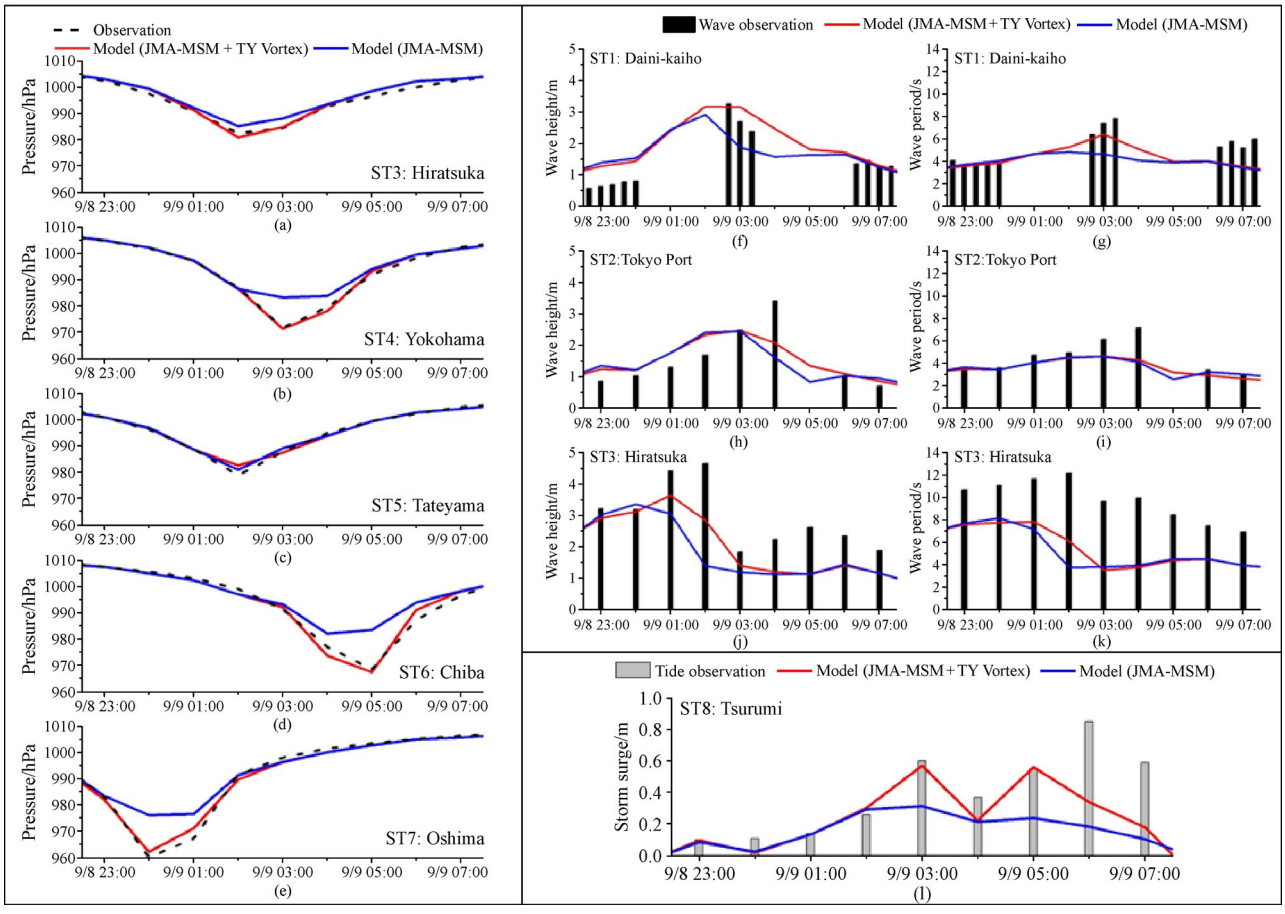

Fig. 6 (a)–(e):Sea-level pressure observed at five meteorological stations and comparisons with simulations from JMA-MSM + TY Vortex and JMA-MSM alone. ST3, ST4, and ST7 are located on the left-hand side of the typhoon course, whereas ST5 and ST6 are on the right-hand side. In particular, the time-series of ST4, ST6, and ST7, nearby the typhoon track, demonstrates close proximity between the observation and JMA-MSM + TY Vortex. (f)–(k): Comparison of significant wave height and period at three locations: inside Tokyo Bay (ST1, ST2) and outside (ST3). (l) Storm surge height at ST8 in Yokohama.

Sagami Bay, it is by far too small to include the broad oceanic basin from where the entire typhoon track was encompassed. Therefore, it is considered that the offshore swell is not adequately reproduced in the numerical model, resulting in the underestimation of the peak wave. Nevertheless, at **ST3**, the tendency of the rising and falling wave is similar between the model and observation. In particular, the feature that the wave height dropped sharply from 2 am to 3 am could also be reproduced in the numerical model. As is clear from Fig. 7, the southward wind was predominant in this time zone, and it seems that the action that pushed the waves back offshore was remarkable. The good estimation for the sudden change in wave direction is likely due to the incorporation of a highly accurate approximation scheme for the nonlinear energy transport term in the SWAN model.

The observed storm surge at Tsurumi (**ST8**), which is located in the northern part of Yokohama, is also presented in Fig. 6. When wave overtopping occurred, the abnormal surge component was 20–60 cm. Although not extreme, this extra rise in water should have contributed to the exacerbation of coastal flooding in Yokohama.

4 Results and discussion

4.1 Estimated wave

Typhoon Faxai traversed almost directly above Tokyo Bay from midnight to dawn on September 9 (Fig. 7). It was reported that coastal inundation due to wave overtopping started around 2:00–2:30 am at Fukuura (**KG3**) in Yokohama City (Suzuki et al., 2020). At that time, the typhoon was about to make landfall at Miura Peninsula; however, the clear eye was still located in Sagami Bay. Therefore, the inundation in Tokyo Bay took place slightly before the typhoon landfall. The estimated wave height at approximately 1 km off Fukuura is 3.4 m. SWAN model cannot take into account wave reflection and splash. This location is considered to be unaffected by reflections. Based on the broken windows on the second floor of a building near the seawall (**KG3** in Fig. 3), however, it can be estimated that the actual waves reached even higher. Strong winds blew toward the coast of Fukuura from the E–SE direction. At 3 am, more intensified winds blew toward Yokohama Port (**KG1**). However, the wind

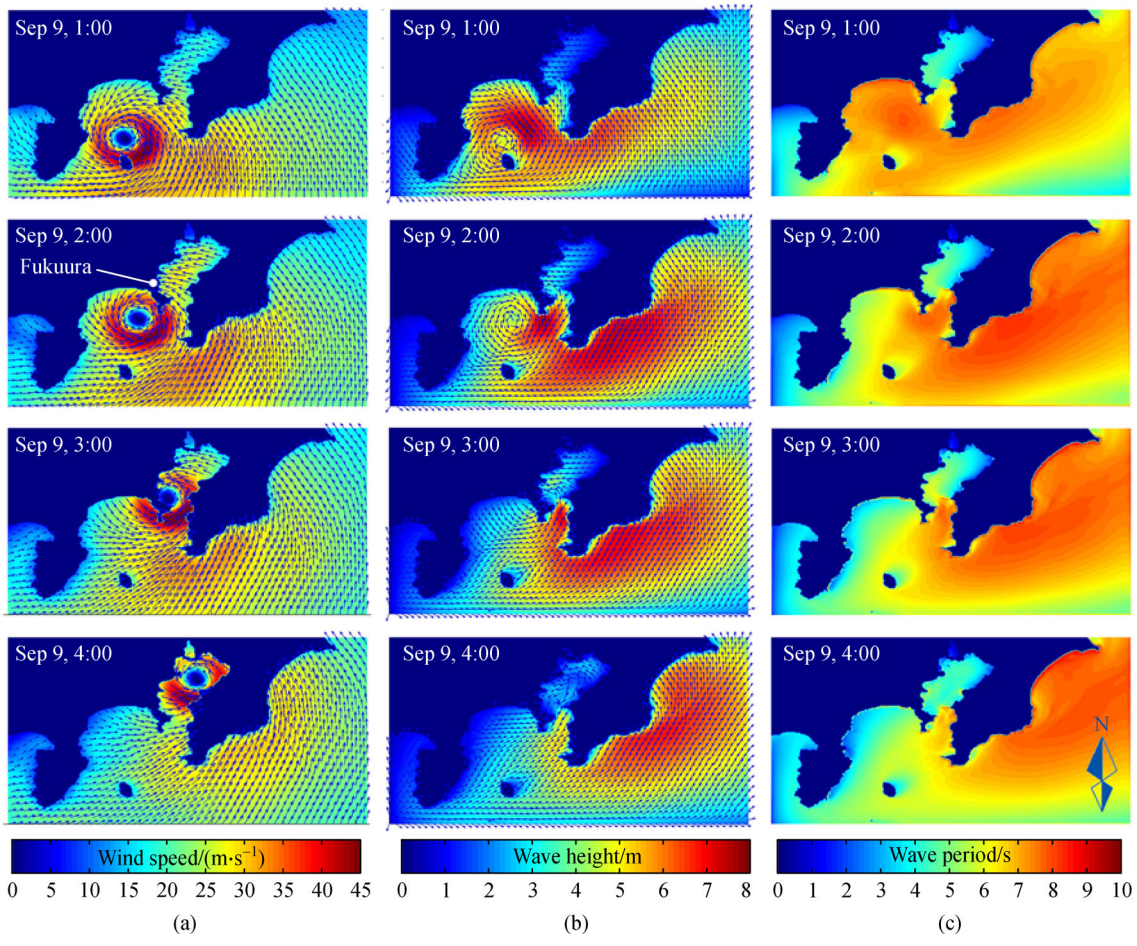

Fig. 7 Simulation output of JMA-MSM + TY Vortex. (a) Wind speed; (b) Wave height; (c) Wave period. Date and time: Japan Standard Time.

suddenly changed its direction toward the side of the Boso Peninsula at 4 am. The sudden change in wind direction is readily attributed to the advancing of the small typhoon. The wind-speed distribution suggests that wind primarily acted along the bay's short axis (east–west). As a result, the wave became particularly high on the west shore of Tokyo Bay. When Faxai traversed over the bay, a high wave also appeared on the east shore of the Boso Peninsula, facing the Pacific Ocean. The wave height at Kujukurihama Beach (**CB3**) was estimated to be over 5 m, and this high wave may have damaged the management facility in the sandy beach, as described in the previous section. In addition, this place faces the Pacific Ocean and is prone to long-period waves. Therefore, the typhoon-induced local wave is considered to unfavorably overlap with the swell, leading to the significant run up on the beach.

4.2 Wave generated within the bay vs. propagated from the outer sea

The inner-bay wave during the typhoon can be accounted for as the sum of two components: fetch-limited waves developed inside the bay and propagated waves from the outer sea. To quantify each contribution, a hypothetical numerical experiment was performed, as shown in Fig. 8. The original case is the same as the condition described in the previous section. In the hypothetical experiment, an artificial object was intentionally placed in order to close Tokyo Bay. To do this, the bathymetry of the bay mouth, approximately 9 km long (A line drawn from east to west, slightly longer than the shortest bay mouth distance of 7 km), was replaced with a null value in the simulation, serving as a breakwater to protect the bay from outer-sea waves. The same wind forcing was input for both the original and hypothetical cases. The analysis focused on the instance at 2 am, when Faxai caused the overtopping waves in Fukuura. A high wave was found to be generated even when the bay is disconnected. In the upper half of the bay, the wave height and period are distributed almost equally in the two cases. However, there is a small discrepancy in the lower half (particularly near the bay mouth), suggesting the influence of propagated waves from the outer sea. Figure 9 shows the percentage contribution of outer-bay waves to the total wave. This map was produced by comparing the wave energy (proportional to the square of the wave height) between the open-bay and closed-bay cases. Near the bay mouth, the outer-bay wave constitutes the majority of the wave energy. However, the contribution tends to drop sharply as the wave propagates into the bay. For example, the

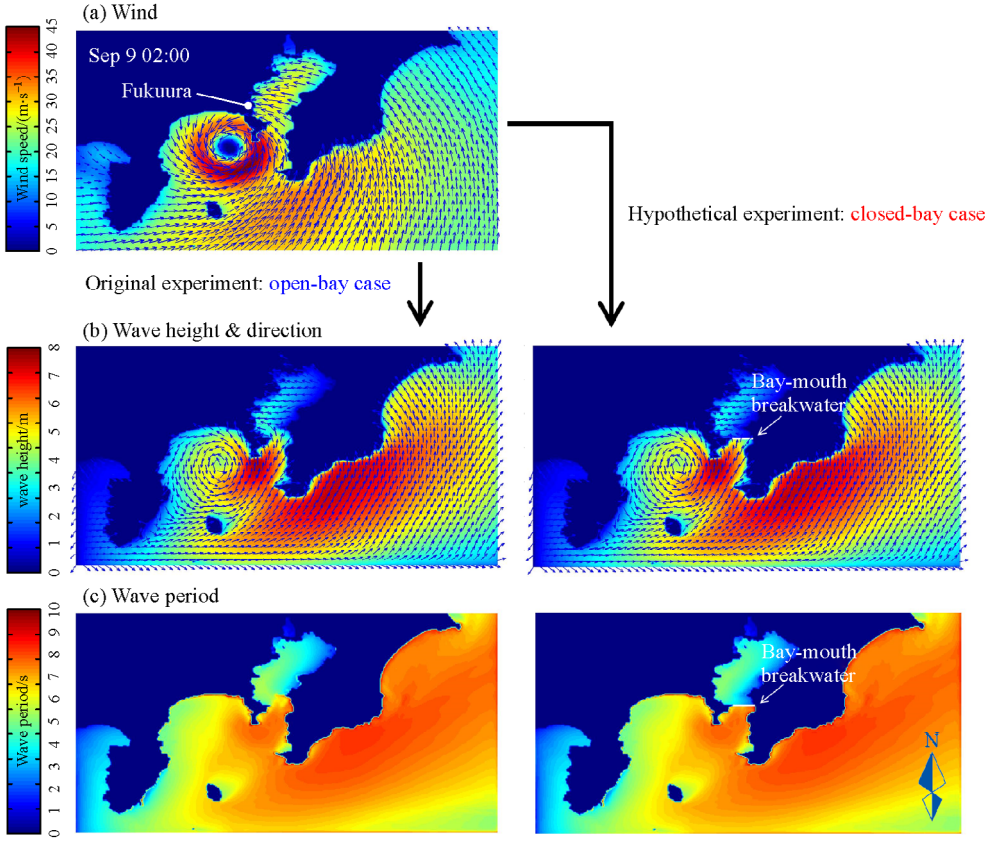

Fig. 8 Numerical experiment for quantifying the contribution of inner-bay waves and outer-sea waves. A hypothetical breakwater is placed in the bay mouth to prevent outer-sea waves from entering the bay. Date and time: Japan Standard Time.

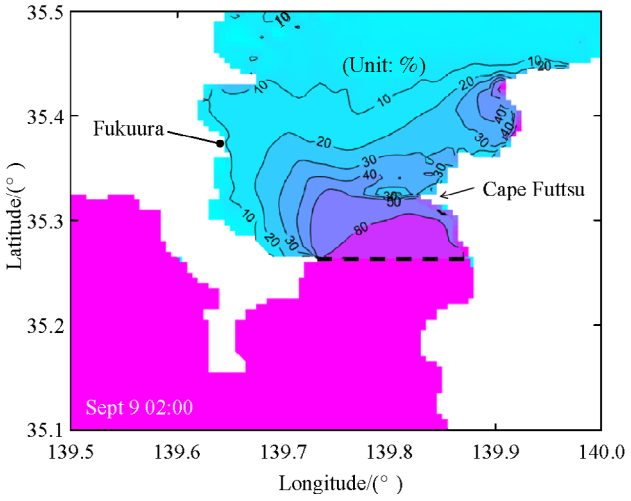

Fig. 9 Percentage of wave energy propagating from the outer sea.

percentage of the contribution is as low as 10%–20% off the coast of Fukuura. The bay is effectively protected by the two peninsulas. In addition, Cape Futtsu, which protrudes into the bay, forms a shallow area that effectively reduces the wave energy. Therefore, it is clear that most of the high waves off Yokohama were of the form of inner-bay-generated fetch-limited waves.

Although not related to the simulation results in Tokyo Bay, it is noticed that the direction of the waves near the offshore boundary in Fig. 8(b) looks a little unnatural. In SWAN model, the offshore boundary conditions effectively absorb waves propagating in a perpendicular direction. However, the direction of waves under the typhoon is complex, and waves propagating parallel to the boundary are not treated precisely.

4.3 Typhoon size and wave energy

The wave concentration off Yokohama can also be identified in Fig. 10(a), which shows the distribution of the maximum wave height during the passage of Faxai. Interestingly, within the bay, the maximum wave occurred on the left-hand side, namely "the navigable semicircle." This is contrary to the general understanding, as the wave in the left half-circle of the typhoon is considered calm, compared with that in the right half-circle, called "the dangerous semicircle" (Uji, 1975). For the outer bay area, in fact, high waves appeared in the dangerous semicircle, reaching as high as 7 m. These waves may have also been energized by the high degree of synchronicity between the waves and the moving storm, referred to as the trapped fetch wave (Bowyer and MacAfee, 2005). As Faxai was a small typhoon (if not the smallest), the high waves were concentrated in a limited area off Yokohama. To investigate the influence of the typhoon size, the authors considered a hypothetical case. In this test, the radius of the maximum wind speed was tripled (i.e., $r_m = 28$ km $\times$ 3) in the TY Vortex model, while the forward speed and typhoon track conditions were maintained (Fig. 10(b)). The triple-sized typhoon is the similar size as Typhoon Hagibis, which occurred in the same year (Table 1). Owing to the enlargement, the wave was also enhanced significantly. The contour line with 3 m extends throughout the bay. This is because the effective wind duration increases as the size of the typhoon increases. In the case of a large typhoon, there are two areas where the wave heights are over 4 m, off Yokohama and off Chiba. The high wave off Chiba is generated by westerly winds that appear in the rear semicircle of the typhoon. The height of the wharf in Tokyo Bay is usually approximately 3 m above sea level.

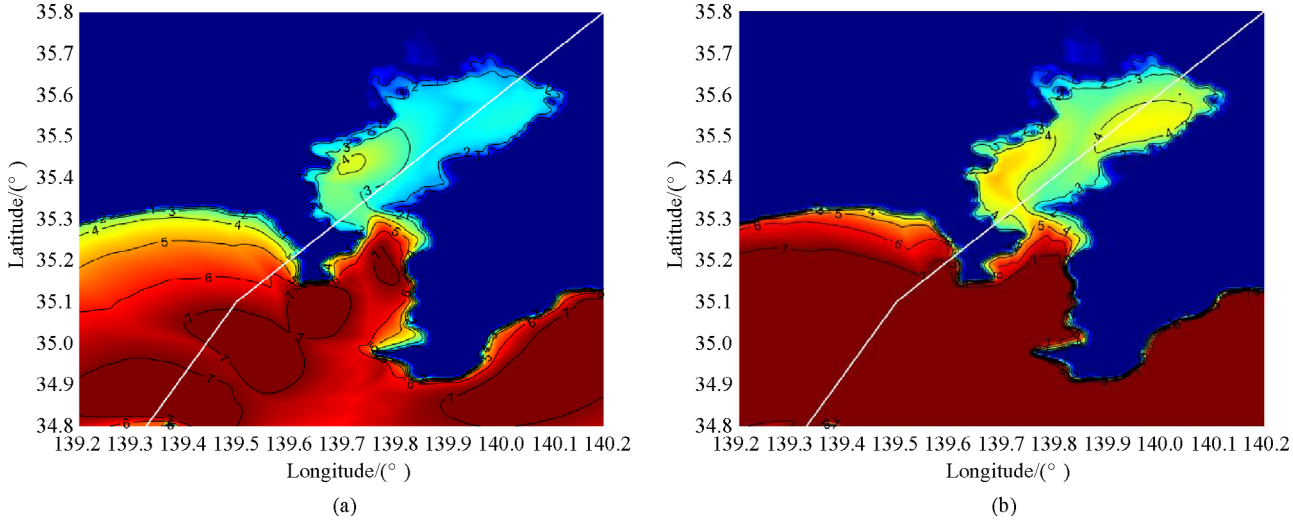

Fig. 10 (a) Maximum wave height inside and outside Tokyo Bay during the passage of Faxai. The white line indicates the typhoon track. In the bay, the maximum wave occurred in the navigable semicircle (left-hand side of the track). (b) Bottom: hypothetical case, in which the size of Faxai was tripled.

Therefore, there is a concern that the high-wave risk may significantly increase when waves exceed 3 m.

If a typhoon is directly translated above Tokyo Bay, waves inevitably propagate in the east–west short-axis direction of the bay. In this case, the east and west coasts of Tokyo Bay are more likely to be hit by high waves. However, wind blowing along the north–south longitudinal axis cannot be underestimated (Hoshino et al., 2016). For example, the worst historical typhoon took place in October 1917, directly hitting Tokyo and its surrounding areas. The storm surge induced by this typhoon claimed 1301 lives while destroying 43083 houses, and a total of 8220 ships were swept away (Omori, 1918). The center of this typhoon passed north-west of Tokyo shortly after midnight, and an abrupt increase in the sea level of Tokyo Bay occurred. At that time, strong winds reportedly blew from the south-south-east. Consequently, seawater was pushed toward the innermost part of Tokyo Bay, generating a high water level of over 3 m above the mean sea level (Arakawa, 1957).

A recent parametric study also suggests that among the many hypothetical tracks, a large typhoon transiting parallel to the longitudinal axis of Tokyo Bay, making landfall approximately 25 km south-west, is found to generate the largest storm surge in the innermost part of Tokyo Bay (Islam and Takagi, 2020a). In this way, if a typhoon with a large radius makes landfall on the west side of Tokyo, it is anticipated that the influence of southerly winds will be more prominent, causing a greater impact on the north end of the bay.

Lastly, the propagation of fully-developed waves into Tokyo Bay is shortly discussed. The purpose of the present numerical analysis is to investigate the rapid development of short-fetch waves caused by typhoons. However, long-period open-ocean waves transmitted from the distant ocean are not adequately reproduced if the computational domain is small (Le et al., 2019). This may be one of the reasons why both wave height and period are underestimated at Hiratsuka (**ST3**), which faces the open sea. According to the Pierson–Moskowitz spectrum, the significant wave height H_{m0} (m) can be calculated for a fully grown sea state, based on wind speed U (m/s), as $H_{m0} = 0.0246U^2$. The JMA has adopted a limit of 17 m/s as the lower limit of wind speed for tropical cyclone. When this wind blows for a long time, the waves develop to approximately 7 m high. Figure 6(k) shows that a wave period of up to 12 s was observed at Hiratsuka (**ST3**). Figure 11 shows the distribution of estimated wave energy in response to an incoming open ocean wave. In this analysis performed with SWAN, waves induced by the typhoon inside the domain are ignored, while a 7 m and 12 s wave is imposed along the three offshore boundaries. The decay of wave energy is particularly significant within Sagami Bay. This can be attributed to the effect of seafloor friction over the shallow water and topographical effects such as capes and islands. Accordingly, the waves reach the shore as a form of swell with a milder waveform gradient. The energy of open ocean waves entering Tokyo Bay is estimated very small, less than 5% of the total energy. This may be the reason why periods longer than 10 s have not been observed in Tokyo Bay, such as Daini-kaiho (**ST1**) and Tokyo Port (**ST2**) (Fig. 6).

5 Conclusions

Immediately after the occurrence of Typhoon Faxai, the

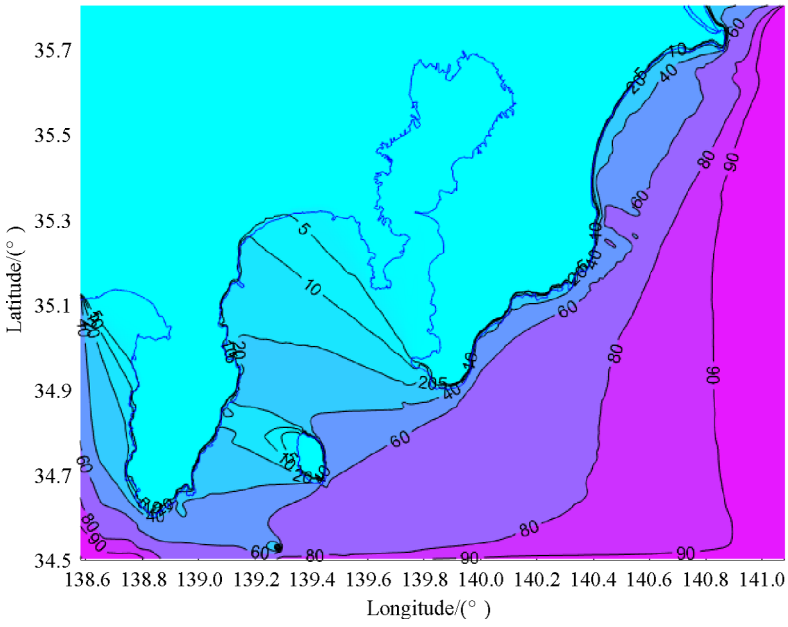

Fig. 11 Percentage of wave energy propagated from the offshore boundaries, where a 7 m and 12 s wave is imposed.

authors investigated the coasts of Kanagawa and Chiba and found that no significant high-wave damage occurred on Sagami Bay, Boso Peninsula, or other coasts facing the Pacific Ocean. However, Yokohama, which faces Tokyo Bay, suffered overtopping waves that crossed upright seawalls. This has raised questions for us about the vulnerability of high waves in Tokyo Bay. Faxai is a strong typhoon that slowly traversed Tokyo Bay, and the main cause of the high waves over 3 m generated in the bay was not the swells from the outer sea but the wind waves that rapidly developed in the bay owing to easterly strong winds, even with such a short fetch (the short-axis distance of Tokyo Bay ranges from 10 to 15 km). Faxai was a small typhoon; however, hypothesizing a radius triple that of Faxai, the wave height would exceed 3 m over the entire bay and surpass 4 m off the coasts of Yokohama and Chiba. With regard to Japan's coastal disaster management for inner-bay areas, protection against storm surges and tsunamis receives the greatest priority. Wind-wave disasters are far less prioritized because the waves in the bay are calm during most of the year. This is also likely because high waves may only cause damage to limited coastal infrastructure and adjacent facilities, rarely causing significant human loss. In the case of Tokyo Bay, the risk of high waves is also overlooked because two peninsulas are believed to serve as a perfect natural breakwater. However, given the importance of waterfronts for economic development high wave risk should not be further underestimated. Once the coastal dike collapses by the force of the high wave, the production activities in the harbor and industrial areas suddenly stop, and the resulting economic damage is immeasurable.

Acknowledgements This research was funded by grants awarded to Tokyo Institute of Technology (Japan Society for the Promotion of Science, Nos.16KK0121, 19K04964 and 19K24677). The authors thank Le Tuan Anh, Rezuanul Islam, Takayuki Sugiu, and Fumitaka Furukawa for their assistance during the post-disaster survey immediately after Typhoon Faxai.

References

Arakawa H (1957). On typhoon storm tides. Geofis Pura Appl, 38(1): 231–249

Booij N, Ris R C, Holthuijsen L H (1999). A third-generation wave model for coastal regions 1. Model description and validation. J Geophys Res, 104(C4): 7649–7666

Bowyer P J, MacAfee A W (2005). The theory of trapped-fetch waves with tropical cyclones—an operational perspective. Weather Forecast, 20(3): 229–244

Bretschneider C L (1951). Revised wave forecasting relationship. Proc. Coastal Engineering Proceedings, 1(2)

Chen W B, Chen H, Hsiao S C, Chang C H, Lin L W (2019). Wind forcing effect on hindcasting of typhoon-driven extreme waves. Ocean Eng, 188: 106260

Cressman G P (1959). An operational objective analysis system. Mon Weather Rev, 87(10): 367–374

Delft T U (2000). SWAN Cycle III Version 40.11 User Manual. 2000

Donelan M, Skafel M, Graber H, Liu P, Schwab D, Venkatesh S(1992). On the growth rate of wind-generated waves. Amosphere-Ocean, 30 (3): 457–478

Hasselmann K F, Barnett T P, Bouws E, Carlson H, Cartwright D E, Eake K, Euring J A, Gicnapp A, Hasselmann D E, Kruseman P, Meerburg A (1973). Measurements of wind-wave growth and swell decay during the Joint North Sea Wave Project (JONSWAP). J German Hydrogr, Reihe A (in German)

Heidarzadeh M, Rabinovich A B (2020) Natural hazards, combined hazard of typhoon-generated meteorological tsunamis and storm surges along the coast of Japan. Nat Hazards, (2020): 1–34

Heidarzadeh M, Takagawa T, Iwamoto T, Takagi T (2021). Field surveys and numerical modeling of the August 2016 typhoon Lionrock along the northeastern coast of Japan: the first typhoon making landfall in Tohoku region. Nat Hazards 105(1): 1–19

Hoshino S, Esteban M, Mikami T, Takagi H, Shibayama T (2016). Estimation of increase in storm surge damage due to climate change and sea level rise in the Greater Tokyo area. Nat Hazards, 80(1): 539–565

Hsiao S C, Chen H, Wu H L, Cehn W B, Chang C H, Guo W D, Chen Y M, Lin L Y (2020). Numerical simulation of large wave heights from Super Typhoon Nepartak (2016) in the eastern waters. J Mar Sci Eng, 8(3): 217

Hwang P A, Walsh E J (2018). Estimating maximum significant wave height and dominant wave period inside tropical cyclones. Weather and Forecasting, 33(4): 955–966

Islam R, Takagi H (2020a). Typhoon parameter sensitivity of storm surge in the semi-enclosed Tokyo Bay. Front Earth Sci, 14 (3): 553–567

Islam R, Takagi H (2020b). Statistical significance of tropical cyclone forward speed on storm surge generation: retrospective analysis of best track and tidal data in Japan. Georisk

Islam R, Takagi H, Anh L T, Takahashi A, Ke B (2018). 2017 Typhoon Lan reconnaissance field survey in coasts of Kanto Region, Japan. J Japan Soc of Civil En, Ser. B3. Ocean Eng, 74(2): 593–598

JMA (2019). Outline of the operational numerical weather prediction. avaible at Japan Meteorological Agency website

Komen G J, Cavaleri L, Donelan M, Hasselmann K, Hasselmann S, Janssen P A E M (1994). Dynamics and Modelling of Ocean Waves. Cambridge: Cambridge University Press

Le T A, Takagi H, Heidarzadeh M, Takata Y, Takahashi A (2019). Field Surveys and numerical simulation of the 2018 Typhoon Jebi: impact of high waves and storm surge in semi-enclosed Osaka Bay, Japan. Pure Appl Geophys, 176(10): 4139–4160

Mitsuyasu H (1972). The one-dimensional wave spectra at limited fetch. In: Proceedings of 13th Conference on Coastal Engineering, Vancouver, Canada

Molitor D A (1935). Wave pressures on sea walls and breakwaters. Trans ASCE, 100: 984

Mori N, Yasuda T, Arikawa T, Kataoka T, Nakajo S, Suzuki K, Yamanaka Y, Webb A (2019). Typhoon Jebi post-event survey of coastal damage in the Kansai region, Japan. Coast Eng J, 61(3): 278–294

Myers V A (1954). Characteristics of United States Hurricanes Pertinent

to Levee Design for Lake Okeechobee, Florida. Hydrometeorological Report, 32. Washington DC: US Government Printing Office

Omori F (1918). Tsunami in Tokyo Bay. Earthquake Investiga, 89: 19–48 (in Japanese)

Pierson W J Jr, Moskowitz L A (1964). Proposed spectral form for fully developed wind seas based on the similarity theory of S. A. Kitaigorodskii. J Geophys Res, 69(24): 5181–5190

Schloemer R W (1954). Analysis and Synthesis of Hurricane Wind Patterns over Lake Okeechobee, Florida. Hydrometerorological Report No.31. Washington DC: US Department of Commerce, Weather Bureau

Solomon R (2016).Tokyo Bay at risk to tsunami. Beacon Reports

Stevenson T (1874). The Design and Construction of Harbours. Cambridge: Cambridge University Press

Suzuki T, Tajima Y, Watanabe M, Tsuruta N, Takagi H, Takabatake T, Suzuki K, Shimozono T, Shigihara Y, Shibayama T, Kawaguchi S, Arikawa T (2020). Post-event survey of locally concentrated disaster due to 2019 Typhoon Faxai along the western shore of Tokyo Bay, Japan. Coast Eng J, 62(2): 146–158

Sverdrup H U, Munk W H (1947). Wind, Sea and Swell: Theory of Relations for Forecasting. Washington: U.S. Navy Hydrographic Office

Takabatake T, Mäll M, Esteban M, Nakamura R, Kyaw T O, Ishii H, Valdez J, Nishida Y, Noya F, Shibayama T (2018). Field survey of 2018 Typhoon Jebi in Japan: Lessons for disaster risk management. Geosciences (Basel), 8(11): 412

Takagi H, Li S, de Leon M, Esteban M, Mikami T, Matsumaru R, Shibayama T, Nakamura R (2016). Storm surge and evacuation in urban areas during the peak of a storm. Coast Eng, 108: 1–9

Takagi H, Wu W (2016). Maximum wind radius estimated by the 50 kt radius: improvement of storm surge forecasting over the western North Pacific. Nat Hazards Earth Syst Sci, 16(3): 705–717

Takagi H, Esteban M, Shibayama T, Mikami T, Matsumaru R, Leon M D, Thao N D, Oyama T, Nakamura R (2017). Track analysis, simulation, and field survey of the 2013 Typhoon Haiyan storm surge. J Flood Risk Manag, 10(1): 42–52

Takagi H, Xiong Y, Furukawa F (2018). Track analysis and storm surge investigation of 2017 Typhoon Hato: were the warning signals issued in Macau and Hong Kong timed appropriately? Georisk, 12(4): 297–307

Takagi H, Islam M R, Anh L T, Takahashi A, Sugiu T, Furukawa F (2020a). Investigation of high wave damage caused by 2019 Typhoon Faxai in Kanto region and wave hindcast in Tokyo Bay, J Japan Soc Civil En, Ser. B3. Ocean Eng, 76(1): 12–21

Takagi H, Tomiyasu R, Oyake T, Araki T, Mori K, Matsubara Y, Ninomiya Y, Takata Y (2020b). Tsunami intrusion through port breakwaters enclosed with self-elevating seawalls. Ocean Eng, 199: 107028

Uji T (1975). Numerical estimation of sea wave in a typhoon are. Rep Meteorol Geophys, 26(4): 199–217

United Nations (2018). 2018 Revision of World Urbanization Prospects. Available at United Nations website

Wilson B W (1965). Numerical prediction of ocean waves in the North Atlantic for December, 1959. Deutsche Hydrographische Z, 18(3): 114–130

Yamamoto H, Kanemitsu N, Miyake Y, Ohtani Y, Watanabe Y, Sakamoto K, Iwaya K (2020). Damage investigation of gust wind and storm surges disasters in Tokyo Bay area by Typhoon No.15 (Faxai) in 2019. J Nat Disaster Sci, 39(2): 113–136

Young I R, Verhagen L A (1996). The growth of fetch limited waves in water of finite depth. Part 1: total energy and peak frequency. Coast Eng, 29(1−2): 47−78